Application of neutron diffraction in analysis of residual stress profiles in the cylinder web region of an as-cast V6 Al engine block with cast-in Fe liners

Sediako, D.; D'Elia, F.; Lombardi, A.; Machin, A.; Ravindran, C.; Hubbard, C.; Mackay, R.

Publisher's version / Version de l'éditeur:
https://doi.org/10.1002/9781118062142.ch37
Supplemental Proceedings: Materials Fabrication, Properties, Characterization, and Modeling, 2, p. 299, 2011-04-19

APPLICATION OF NEUTRON DIFFRACTION IN ANALYSIS OF RESIDUAL STRESS PROFILES IN THE CYLINDER WEB REGION OF AN AS-CAST V6 Al ENGINE BLOCK WITH CAST-IN Fe LINERS

D. Sediako[1], F. D'Elia[2], A. Lombardi[2], A. Machin[2], C. Ravindran[2], C. Hubbard[3], R. Mackay[4]

[1]Canadian Neutron Beam Centre – National Research Council of Canada – Chalk River Laboratories; Chalk River, ON, K0J 1J0, Canada
[2]Centre for Near-net-shape Processing of Materials, Ryerson University; 101 Gerrard St. E; Toronto, ON, M5B 2K3, Canada
[3]Oak Ridge National Laboratory; 1 Bethel Valley Road; Oak Ridge, TN 37831, USA
[4]Nemak Canada; 4600 G.N. Booth Drive; Windsor, ON, N9C 4G8, Canada

Keywords: 319 aluminum alloy, engine block, sand casting, neutron diffraction, residual stresses, microstructure, hardness.

Abstract

Continuous efforts to develop a lightweight alloy suitable for the most demanding applications in automotive industry resulted in a number of advanced aluminum (Al) and magnesium alloys and manufacturing routes. One example of this is the application of 319 Al alloy for production of 3.6L V6 gasoline engine blocks. Aluminum is sand cast around Fe-liner cylinder inserts, prior to undergoing the T7 heat treatment process. One of the critical factors determining the quality of the final product is the type, level, and profile of residual stresses along the Fe liners (or extent of liner distortion) that are always present in a cast component.

In this study, neutron diffraction was used to characterize residual stresses along the Al and the Fe liners in the web region of the cast engine block. The strains were measured both in Al and Fe in hoop, radial, and axial orientations. The stresses were subsequently determined using generalized Hooke's law. Further, optical microscopy and hardness measurements were performed from top to bottom along the interbore region of each cylinder. The results indicate that a variation in cooling rate along the cylinder caused a refinement of dendrites at the bottom of the cylinder, resulting in increased hardness.

This study gives invaluable insight on anticipated service properties of the engine block and demonstrates that neutron strain mapping is an efficient tool for optimization of manufacturing technologies.

Introduction

Aluminum (Al) alloys are increasingly popular in the automotive and aerospace industries, due to their low density, excellent strength and good castability. One of the most widely used Al alloys is the aluminum-silicon-copper (Al-Si-Cu) system. These alloys benefit from Cu additions, which contribute to strengthening and machinability and Si additions, which improve castability. Aluminum alloy 319 is the most frequently used Al-Si-Cu alloy. Common applications of this alloy include transmission cases, cylinder heads and engine blocks.

Engine blocks manufactured by 319 require the use of grey iron (Fe) liners to resist wear from sealings mounted in pistons. These liners are often cast-into the block, which allows for high productivity [1]. However, these cast-in iron liners may pose a problem. During casting, molten Al solidifies around the gray iron liners at the interbore regions. As a result, a significant variation in cooling rate may occur in these regions, leading to a non-uniform microstructure and mechanical properties. This lack of uniformity in microstructure and mechanical properties may lead to further problems when the engine blocks are heat treated and subsequently exposed to service conditions. For instance, a non-uniform microstructure along the engine block may result in a more complete dissolution of equilibrium phases in certain sections of the engine block. This non-uniform dissolution of phases can further result in a variation of material strength and lead to dimensional distortion when the engine blocks are exposed to service conditions [2]. Therefore, there is a need to characterize the microstructure along the cylinder of the engine block, specifically at the interbore regions. Further, residual stress measurements at these regions will enable a quantification of the severity of distortion.

Investigation of the cause of the distortion in the V6 engine block was the focus of this study. Neutron diffraction was carried out to characterize residual stresses along the Al and the Fe liners in the web region of the cast engine block. The strains were measured both in Al and Fe in hoop, radial, and axial orientations, thereby enabling the stresses to be determined using generalized Hooke's law. Detailed microstructural characterization was correlated with the hardness measurements for the engine block from the top of the cylinder bridge to the bottom.

Neutron Stress Analysis

Hoop Strain Mapping

The as-cast engine block was positioned on the sampling table as shown in Figure 1. Figure 1(a) shows the image generated by the spectrometer's control system for measurements of strains in Al and also in Fe liners in the cylinders' web area. The measurements were performed in the web between cylinders 6 and 4 on one side of the V-type engine block. The actual hoop-strain setup is shown in Figure 1(b). The sample was positioned on the table with an over-all precision of +/-0.5 mm.

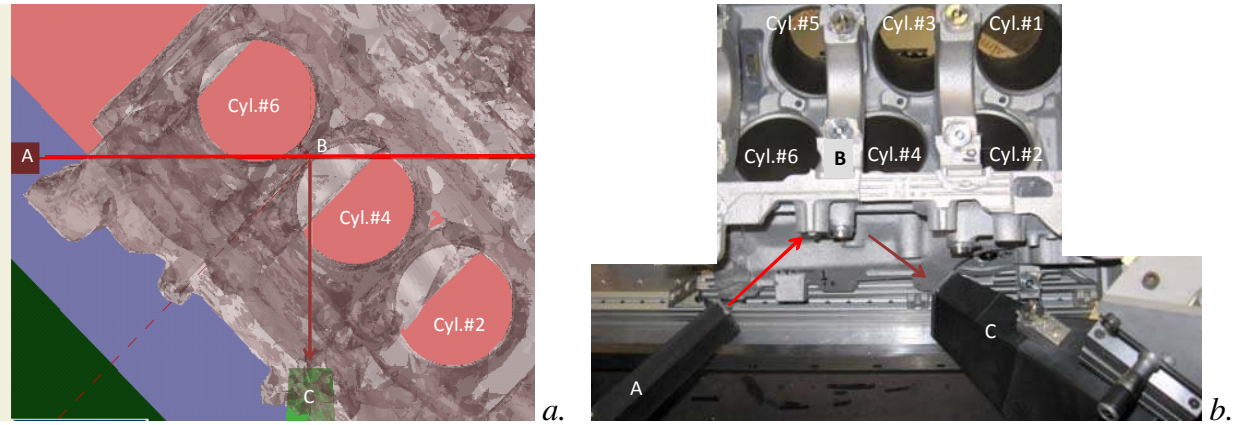

a. *b.*

Figure 1. Orientation of incident and scattering beams and the engine block in measurement of hoop component of strain in the cylinder web region *a* – control system map; *b* – actual positioning of the engine block on the spectrometer sample table.

The selected neutron wavelength for the experiment was 1.73 A. According to Bragg's law, this corresponds to the diffraction angle 2θ of 90.1 degrees for Al (using the 311 planes for Al 319)

and 95.4 degrees for Fe (211 reflection for gray iron). The monochromated incident beam from the reactor-side slit system (A, Figure 1) penetrates through the bulk of the sample material (both Al and Fe). The sampling volume (B) is then formed by the intercept of the incident beam A and diffracted beam that reaches the neutron detector through the slit system C.

After collecting the neutron data at a specific location in the cylinder web the engine was translated in XYZ directions so that the next point-of-interest was positioned in the location of the sampling volume B. The neutron scan was then repeated for the new point. The measured position of the diffracted peak was converted to the interatomic *d*-spacing and then to the values of strain. The reference value of the *d*-spacing for a stress-free material, d_0, was determined by neutron scans of "match stick" samples cut from a low-stress area of the casting. Special care was taken not to introduce any extra stress into the sample material during the machining operation. It was assumed that any residual stress in the material would be relieved during machining of the tiny (2x2x20 mm) stress-free samples. Correspondingly, d_0 values determined for Al was 0.12 nm (1.22 A) and 0.117 nm (1.17 A) for Fe.

The values of hoop strain both for Al web between the cylinders and Fe liners were plotted against Z-coordinate – that is along the cylinder liners – to the depth of 79 mm (Figure 2). The top of the cast-in Fe liners corresponds to the position of 10 mm of Z coordinate; hoop strain in Fe was measured at this position in both liners. As follows, all the strains were tensile, ranging from ~650 to 900 microstrain (or $strain \cdot 10^6$) in the top part of the Fe liners and from 1200 to 1450 microstrain in Al along the web.

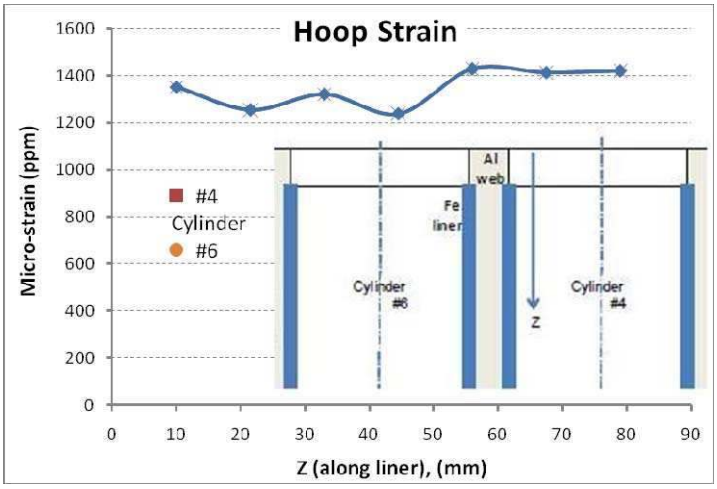

Figure 2. Hoop strains in Al casting and Fe liners along the web region.

Radial Strain Mapping

Similar to that of the hoop strains, the radial-orientation strains were determined in the casting. Figure 3 depicts positioning of the engine block on the sample table.

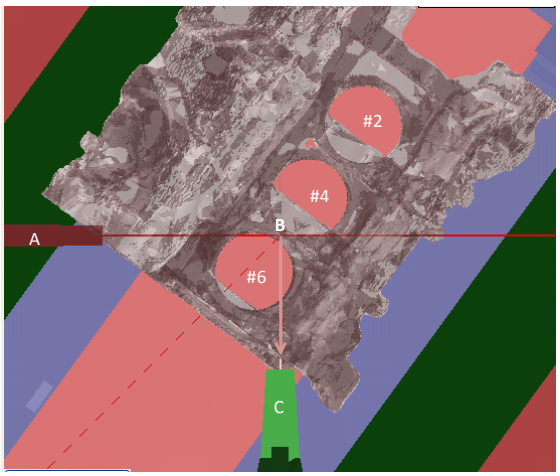

a.
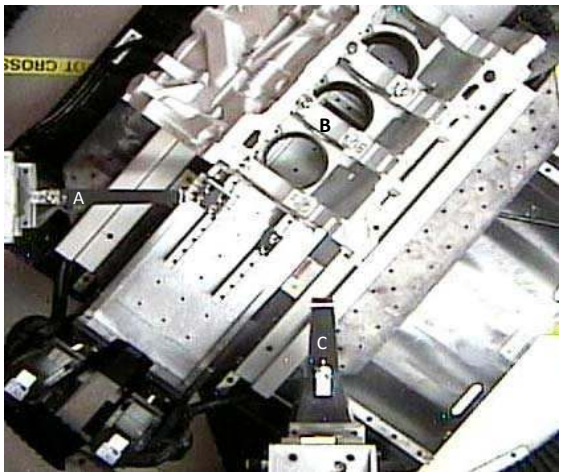

b.

Figure 3. Orientation of incident and scattering beams and the engine block in measurement of radial component of strain in the cylinder web region; *a* – control system map; *b* – actual positioning of the engine block on the spectrometer sample table.

It follows from Figure 4, that Fe liners experienced tensile strain of 1200~1500 $x10^{-6}$, (1200~1500 microstrain) while the strains in Al were compressive and very low in value, ranging from 0 to 400 x 10^{-6} (or 0 to 400 microstrain).

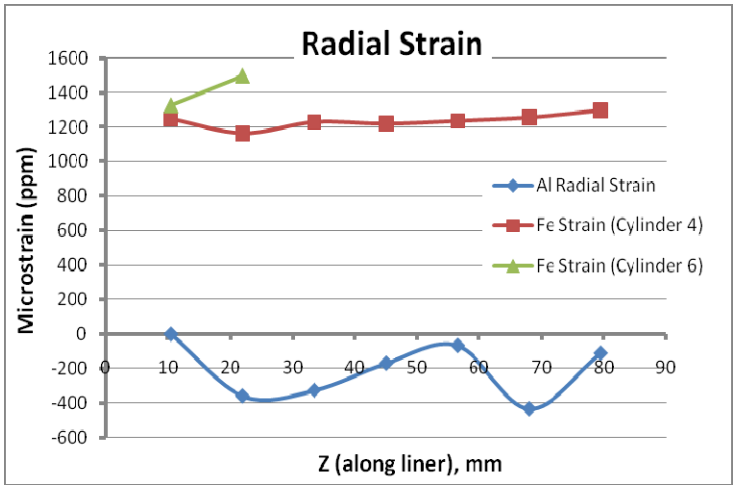

Figure 4. Radial strains in Al casting and Fe liners along the web region.

Axial Strain Mapping

Axial strain mapping completed the 3D characterization of strains in the web region. Figure 5 depicts positioning of the engine block on the sample table.

The results of these measurements are presented in Figures 6. Two web regions were examined in this part of the study; namely, between the cylinders #4 and #6 (1st Web) and, also, between the cylinders #2 and #4 (2nd Web). The purpose of the second web scan was to compare the results received for the two web regions and confirm (or deny) whether both were experiencing similar strain conditions.

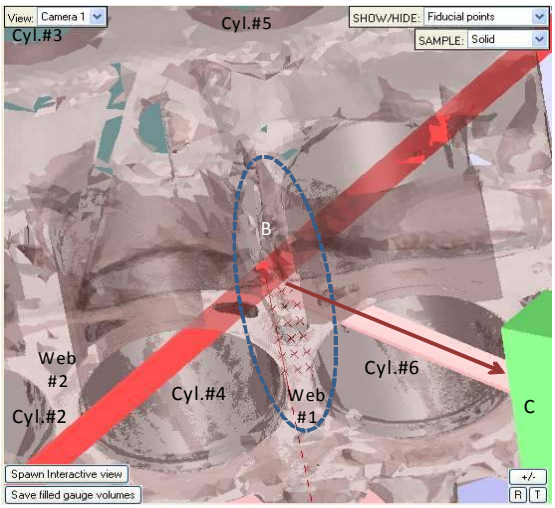

a.

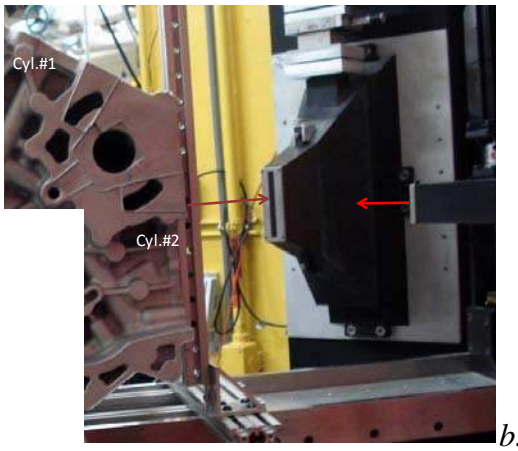

b.

Figure 5. Orientation of incident and scattering beams and the engine block in measurement of axial component of strain in the cylinder web region; *a* – control system map; *b* – actual positioning of the engine block on the spectrometer sample table.

It follows from Figure 6 that axial strain in Al was similar in both cases, although the magnitude of the strain was lower for the second web. The values of strain were tensile and typically ranging from 400 to 1200 microstrain. The lowest value was found at the very top of the web where the strain was slightly compressive with a value of approximately 400 microstrain. Axial strains for the Fe liners, on the other hand, were lower. The values were found to be less than 500 microstrain and were both tensile (1st Web) and compressive (2nd Web). The very top of the Fe liners was under compressive strain reaching approximately 1700 microstrain.

The variation in strain magnitude between the cylinder bridges was expected due to the complex casting geometry of the engine block and thermal gradients existing within the cast engine block. Furthermore, a similar reduction in strain magnitude from the 1st Web and the 2nd Web was observed for the Fe liners as well. Lastly, strain was found to increase at ~10 mm along the cylinder liner in Al and the Fe liners for both webs. This suggests that this region (i.e., top 20 mm of the cylinder liner) may be a critical location for distortion susceptibility.

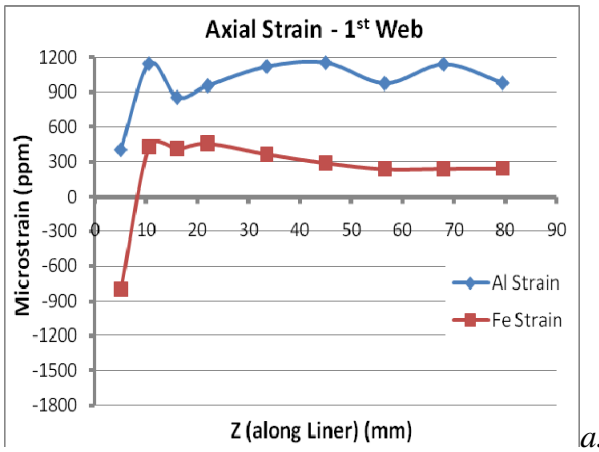

a.

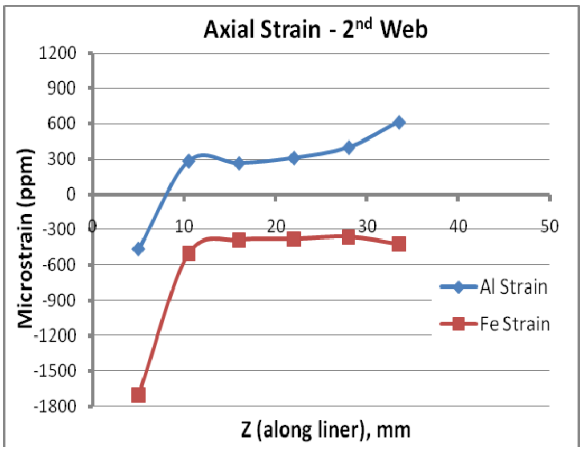

b.

Figure 6. Axial strains in Al casting and Fe liners along web region; *a* – 1st web; *b* – 2nd web.

Residual Stress Analysis

The approach used in this study for determining the three components of strain (hoop, radial, and axial) allows for characterization of residual stress by applying the generalized Hooke's law. Results of these calculations for Fe liners are presented in Figure 7. It follows that residual stresses in Fe liners are ranging from 120 to 180 MPa for all orientations.

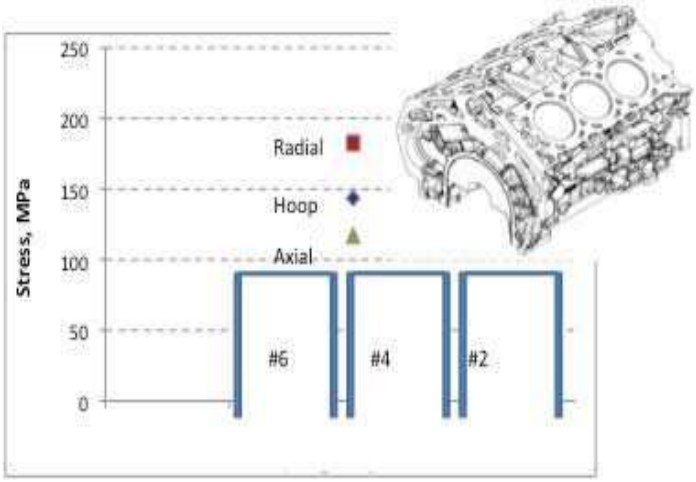

Figure 7. Stress components for the top of iron liner (measurements performed in cylinder #4).

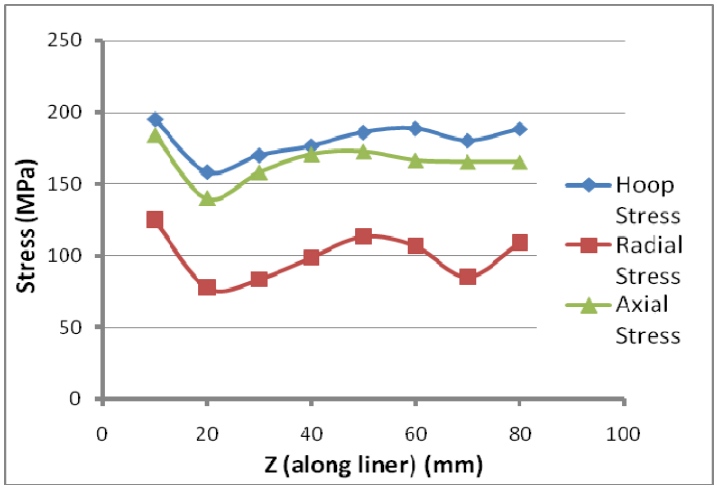

Figure 8. Stress distribution in aluminum along the cylinder web.

Residual stresses for Al are shown in Figure 8. The values of residual stress were slightly higher for Al in comparison to Fe. For instance, hoop stress reached about 190 MPa along the liners to the maximum depth measured of 79 mm, while axial stresses had values near 160 MPa. The values were lower for the radial component of stress, however, as the stress was found to be approximately 100 MPa. All stresses measured in Al and Fe were tensile.

The typical yield stress values for cast iron and 319 aluminum are in the range of 138 – 414 MPa [5] and 96-124 MPa [5, 6], respectively. As a result, the values of residual stress obtained from neutron scans (see Figures 7 and 8) suggest that distortion of Fe liners and Al may occur. In particular, the measured stress values for Al exceed the alloy's yield stress and approach the alloy's tensile strength (~165 MPa [6]). This suggests that high tensile stresses develop in the Al,

which thereby may result in dimensional distortion of the cylinder bores. Furthermore, similar to the axial strain distribution, the distribution of residual stress along the cylinder (Figure 8) illustrates a reduction in hoop, radial and axial stress at ~20 mm along the cylinder liner. In turn, this suggests that the top 20 mm of the cylinder is likely most prone to distortion.

It was reported in [7] that an increase in heat-treating temperature caused bulk strains to go from tensile to slightly tensile or compressive. This gives reason to believe that precipitation of phases (e.g., Cu, Mg) during heat treatment may also play a role in stress development and subsequent engine block distortion. Therefore, it will be beneficial to extend neutron diffraction analysis to heat treated engine blocks.

It is also worthwhile to perform neutron studies to include dyno-tested and service-tested engine blocks as well. This will enable a characterization of residual stresses for these conditions and determine whether distortion of cylinder bores has occurred.

Metallographic Analysis

The composition of the modified 319 Al alloy is shown in Table I. Optical microscopy was carried out on the engine block at the bridge between each cylinder bore, as shown in Figure 9(a). The cylinder bridge was selected for analysis since this location was designated as an area prone to high residual stresses [1]. Microstructural analysis was also performed at various sections (top, upper middle, lower middle, and bottom) along the cylinder, as shown in Figure 9(b). All the cylinder sections analyzed were approximately 15 mm in length. The top and bottom sections were taken approximately 10 mm from the top and bottom, respectively, corresponding to the locations where the Al is in contact with the gray cast iron cylinder liner. Lastly, hardness testing was performed at the top and bottom of each cylinder bridge to relate the mechanical properties to any variation in microstructure.

Table I. Composition of the Modified 319 Aluminum Engine Block (wt %)

Si	Cu	Zn	Fe	Mg	Mn	Ti	Ni	Cr	Sr	Sb	B	Bi	Al
8.5	2.7	0.5	0.4	0.35	0.35	0.15	0.04	0.03	0.005	0.002	0.001	0.001	Bal

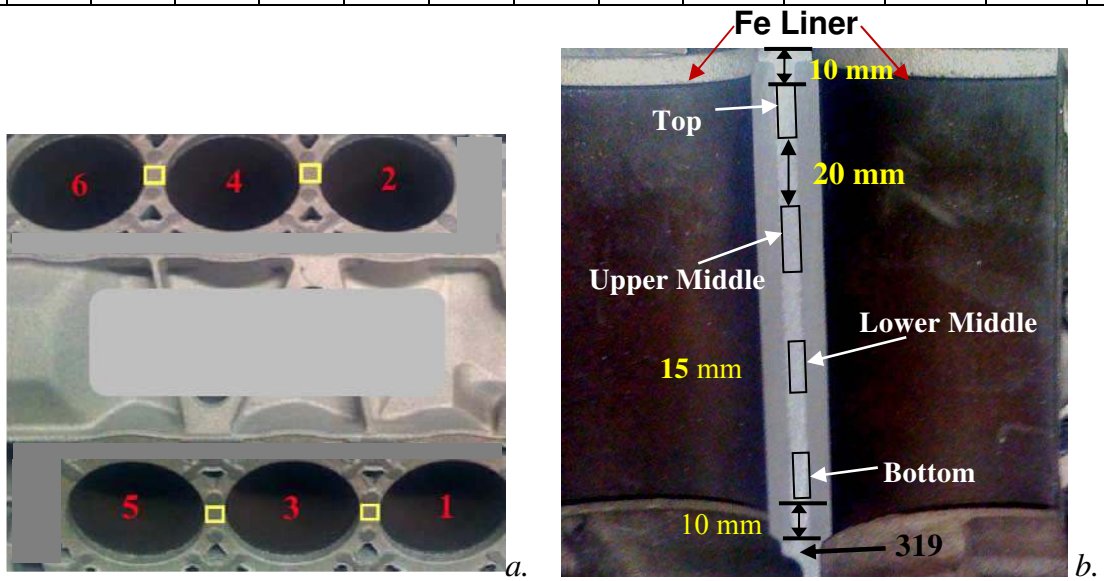

a. *b.*

Figure 9. Images of: (a) engine block illustrating locations of sectioned microscopy samples, (b) cross-section of the cylinder bridge showing sections analyzed along the cylinder depth.

Dendrite Structure

Optical microscopy revealed a significant variation in the dendrite structure of each cylinder bridge when comparing the top and bottom sections of the cylinder. It was observed that the top of the cylinder bridge contained relatively coarse dendrites, while the bottom of the cylinder contained finer dendrites. This is shown in Figure 10.

The secondary dendrite arm spacing was measured at the top, upper middle, lower middle and bottom sections of the cylinder bridge. The results are shown in Figure 11. The measurements confirm the observations in Figure 10, as the SDAS was found to continuously decrease from the top to the bottom of the cylinder.

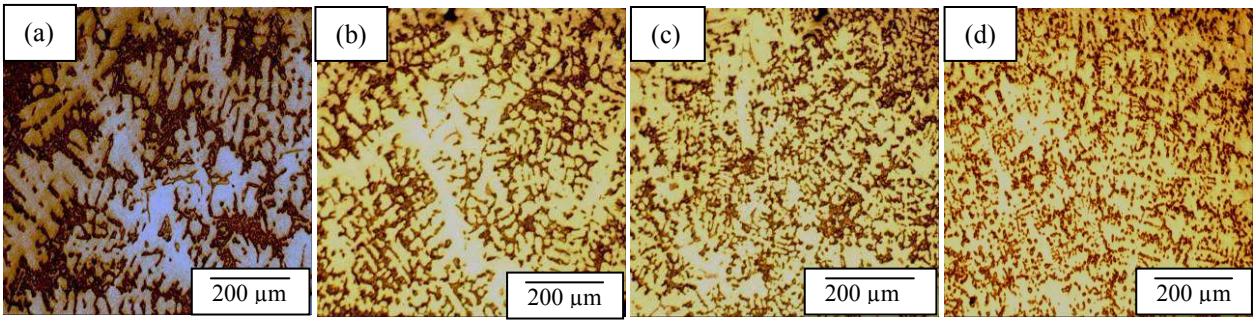

Figure 10. Dendrite structure of Cylinder (2-4) bridge at: (a) top, (b) upper middle, (c) lower middle, and (d) bottom.

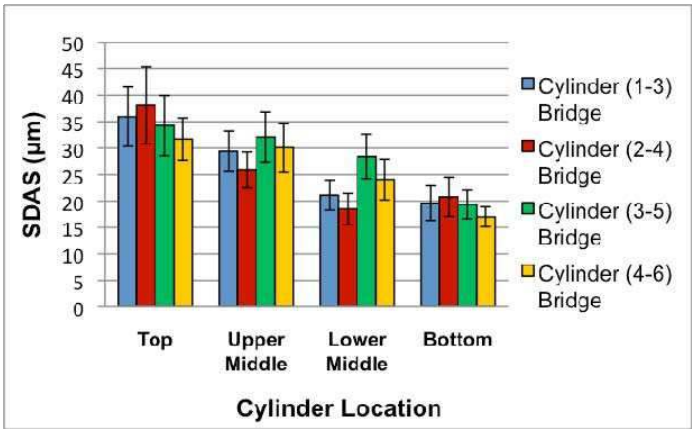

Figure 11. Results of SDAS measurements in the as-cast 319 engine block.

The refinement of dendrites in the bottom section of the cylinder bridge indicated that this section may have experienced a shorter local solidification time and faster cooling rate than the top section [8, 9]. The cooling rates (R) were estimated from the SDAS measurements using an empirical relationship developed by Vazquez-Lopez *et al.* [10] for Al-Si alloys. This relation is shown in Equation 1.

$$SDAS = 36.1R^{-0.34} \quad (1)$$

The cooling rate was estimated to be approximately 1 °C/s at the top of the cylinder and 7 °C/s at the bottom. This result was expected however, based on the design of the sand mould. The bottom section of the cylinder had chills inserted into the sand mould prior to pouring, resulting

in an increased solidification rate. Conversely, the top section of the cylinder was the section nearest to the riser and this section is required to solidify last in order to reduce shrinkage porosity [9]. Therefore, the top section of the cylinder likely had a longer local solidification time, resulting in significantly larger dendrites as compared to the bottom cylinder section.

Hardness Testing

Hardness measurements were performed at the top and bottom locations of the cylinder bridge. The results, in Figure 12 (a), show that there was a small increase in hardness at the bottom of the cylinder. This was likely attributed to the refinement of the dendrites, as microhardness measurements (Figure 12 (b)) showed a negligible change in hardness of the α-Al matrix.

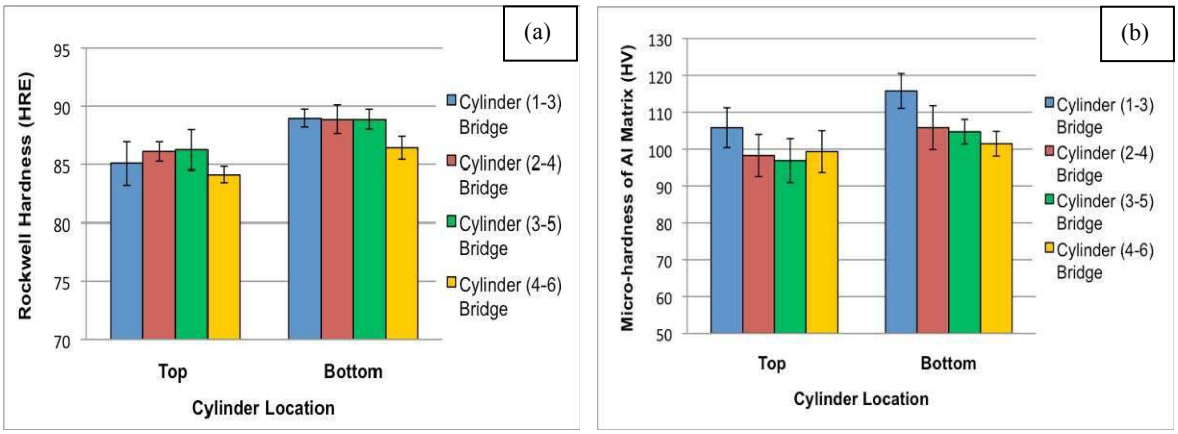

Figure 12. Measurements of (a) Rockwell hardness at the cylinder bridge region, and (b) Vickers microhardness of the Al-matrix in the cylinder bridge region

The increase in hardness indicates increased alloy strength at the bottom of the cylinder compared to the top. Since tensile residual stresses are formed at the Al-Fe interface during solidification, the weaker section of the cylinder would be more prone to dimensional distortion while the engine is exposed to in-service conditions. The results obtained from neutron diffraction analysis support this claim as a drop in hoop, radial and axial residual stress was observed at the top section of the cylinder bridge. The residual stress distribution was not measured at the bottom section due to clearance issues. Nevertheless, the stress measurements show a gradually increasing trend towards the bottom of the cylinder. The increasing stress indicated that dimensional changes, due to the residual stresses generated at the Al-Fe interface, would likely not occur at the bottom of the cylinder. While dimensional distortion may occur when residual stresses surpass the yield point of the material, the residual stresses are partially relieved at locations where permanent deformation has occurred, thus revealing the locations which are prone to distortion [11]. As a result, it can be deduced that the increased alloy strength at the bottom reduced the likelihood of dimensional distortion at this section of the cylinder.

Conclusions

1. Neutron diffraction was applied for strain and stress measurements on an as-cast aluminum V6 engine block in hoop, radial, and axial orientations. Studies were performed for the cylinder web region for iron liners and aluminum to the depth of 79 mm. It was confirmed that all residual stresses in the specified location of the casting are tensile. Stress values are about 180 MPa for iron and typically under 200 MPa for aluminum.

2. Values of stress in Al were found to exceed the alloy's yield stress and approach its ultimate tensile strength. This suggested that a high build up of stress in the Fe liners and Al occurs, which thereby may lead to dimensional distortion. Further investigation is warranted to characterize the residual stresses in the engine block following the T7 heat treatment process. Further, the impact of variations in casting practice (eg. cooling/solidification rate) on grain size and stress level is envisaged for future studies.
3. Microstructural analysis revealed finer dendrites and a subsequent smaller SDAS for the bottom section of the cylinder bridge in comparison to the top. This was attributed to a variation in cooling rate from top to bottom.
4. Rockwell hardness was found to increase by a small amount at the bottom of the cylinder due to the dendrite refinement. This was in correlation to the results obtained from neutron diffraction analysis, as the increased hardness suggested increased alloy strength at the bottom of the cylinder relative to the top, and therefore, a reduced likelihood of distortion for the bottom of the cylinder.

Acknowledgements

The authors are grateful to AUTO21 Network of Centres of Excellence and the Natural Sciences and Research Council of Canada (NSERC) for their financial support. Studies at the 2nd Generation Neutron Residual Stress Mapping Facility at the High Flux Isotope Reactor was partially sponsored by the Department of Energy, Office of Energy Efficiency and Renewable Energy, Vehicle Technologies Program, through the Oak Ridge National Laboratory's High Temperature Materials Laboratory User Program and by the Scientific User Facilities Division, Office of Basic Energy Sciences, U.S. Department of Energy. Neutron stress analysis was completed at CNBC, NRC Canada, under the grant of NSERC. Further, the authors are thankful to Nemak Canada and the members of the Centre for Near-Net-Shape Processing of Materials at Ryerson University.

References

1. E. Carrera, A. Rodríguez, J. Talamantes, S. Valtierra and R. Colás, "Measurement of Residual Stresses in Cast Aluminum Engine Blocks," *Journal of Materials Processing Technology*, 189 (2007), 206-210.
2. M. Li, R. Vijayaraghavan, C. Wolverton, J. Allison, "Simulation of Local Microstructures and Thermal Growth of a Cast 319 Aluminum Alloy Component" (Paper presented at the 1st International Symposium on Metallurgical Modelling for Aluminum Alloys, Pittsburgh, Pennsylvania,13 October 2003).
3. Ismail C. Noyan, Jerome B. Cohen, *Residual Stress: Measurement by Diffraction and Interpretation* (New York, NY: Springer-Verlag, 1987).
4. Jian Lu, ed., *Handbook of Measurement of Residual Stresses* (Lilburn, GA: Fairmont Press, 1996).
5. Eugene Avallone, Theodore Baumeister III, and Ali Sadegh, *Marks' Standard Handbook for Mechanical Engineers 11th Edition* (New York: NY: McGraw-Hill Companies, Inc., 2007).
6. J.R. Davis, ed., *ASM Specialty Handbook: Aluminum and Aluminum Alloys* (Materials Park, OH: American Society for Metals, 1993).
7. D.J. Wiesner, T.R. Watkins, T.M. Ely, S. Spooner, Hubbard and J.C. Williams, "Residual Stress Measurements of Cast Aluminum Engine Blocks using Diffraction", *JCPDS – International Centre for Diffraction Data, Advances in Analysis*, 48 (2005), 136-142.

8. Merton C. Flemings, *Solidification Processing* (New York, NY: McGraw-Hill Companies, Inc., 1974).
9. John Campbell, *Castings* (Oxford, England: ElsevierButterworth-Heinemann, 1991).
10. C. Vazquez-Lopez, A. Calderone, M.E. Rodriguez, E. Velasco, S. Cano, R. Colas, and S. Valtierra, "Influence of Dendrite Arm Spacing on the Thermal Conductivity of an Aluminum-Silicon Casting Alloy", *Journal of Materials Research*, 15 (2000), 85-91.
11. G. Totten et al., eds., Handbook of Residual Stress and Deformation of Steel, (Materials Park, OH: ASM International, 2002).